Discovery and geological significance of Upper Jurassic seismites in the Chiclayo region of Northern Peru

Junan Liu[1], *Weimin Guo[1], Zheng Duan[1], Igor Astete Farffa[2], Fredy Jaimes Salcedo[2], *Yong Zeng[1,]

1. Nanjing Center, China Geological Survey（CGS）, Nanjing 210016, Jiangsu, China
liuja@mail.cgs.gov.cn; mwguo@163.com, dz19882010@163.com, larryzeng @163.com
2.Instituto Geológico Minero y Metalúrgico（INGEMMET）, Lima 15074, Peru
igorastete@ingemmet.gob.pe, fjaimes@ingemmet.gob.pe

**Corresponding author: mwguo@163.com. larryzeng@163.com*

Abstract. Seismites constitute a distinct category of sedimentary rocks that preserve soft-sediment deformation structures and associated seismogenic features, serving as critical stratigraphic archives for reconstructing paleoseismic events and regional tectonic evolution. Accurately identifying seismic sediment deformation structures and distinguishing these earthquake-induced features remains challenging. The Chiclayo region in northern Peru is located at the collision front between the Nazca and South American plates, a place with intense seismic activity. Comprehensive geological studies and section measurements were conducted in the Mesozoic La Leche Formation, identifying abundant brittle and soft-sediment deformation structures classified here as seismites. Five seismic events were determined. The paleogeographic environment of the La Leche Formation corresponds to a Late Jurassic littoral-shallow marine shelf within an initial back-arc basin. Synsedimentary fault activity between Peru's northern coastal plain and western coastal range triggered basin margin collapses. This study provides new insights into Mesozoic plate tectonics in the eastern Pacific and modern seismic impacts on geological environments.

Keywords: Seismites; Soft sediment deformation structures; La Leche formation; Chiclayo region; Peru.

Resumen. Descubrimiento e importancia geológica de las sismitas del Jurásico Superior en la región de Chiclayo, norte de Perú. Las sismitas constituyen una categoría distinta de rocas sedimentarias que conservan estructuras de deformación de sedimentos blandos y rasgos sismogénicos asociados, sirviendo como archivos estratigráficos de importancia para reconstruir eventos paleosísmicos y la evolución tectónica regional. Identificar con precisión las estructuras de deformación sísmica en los sedimentos y distinguir estos rasgos inducidos por terremotos sigue siendo un reto. La región de Chiclayo, en el norte de Perú, está situada en el frente de colisión entre las placas de Nazca y Sudamericana y está caracterizada por una intensa actividad sísmica. Se realizaron estudios geológicos exhaustivos y mediciones de secciones en la Formación La Leche, de edad mesozoica, donde se identificaron abundantes estructuras de deformación frágil y estructuras de deformación de sedimentos blandos, cuyas características indican que se tratan de seismitas. Se determinaron al menos cinco eventos sísmicos. El entorno paleogeográfico de la Formación La Leche corresponde a una plataforma litoral-marina somera del Jurásico Tardío dentro de una cuenca de antearco. La actividad tectónica sinsedimentaria entre la llanura costera septentrional y la cordillera costera occidental de Perú desencadenó el colapso de los márgenes de la cuenca. Este estudio provee nuevos antecedentes sobre la tectónica mesozoica de las placas del Pacífico oriental y las repercusiones sísmicas modernas en los ambientes geológicos.

Palabras clave: *Sismitas; Estructuras de deformación de sedimentos blandos; Formación La Leche; Región de Chiclayo; Perú.*

1. Introduction

Earthquake activity is a key driver of geological evolution, with seismites serving as critical archives of paleoseismic events. These sedimentary structures provide diagnostic markers for reconstructing crustal dynamics, stratigraphic correlations, and ancient tectonic settings (*e.g.,* Seilacher, 1969; Cita et al., 1984; Van Loon, 2014). Global studies over the past four decades have identified seismites across tectonic regimes from the Paleoproterozoic to modern times (*e.g.,* Gong, 1988; Song, 1988; Brogi et al., 2018; Serkan et al., 2019; Esther et al., 2022; Walaa et al., 2022), documenting soft-sediment deformation structures (SSDS) under different tectonic environments (*e.g.,* Owen et al., 2010; Levi et al., 2018; Buchner et al., 2020; Yuan et al., 2022). Significant advances include establishing criteria for sedimentary sequences and triggering mechanisms, such as synsedimentary faulting and volcanic activity (*e.g.,* Hilbert-Wolf et al., 2010; Max et al., 2023; Berra, 2024). These frameworks underpin modern analyses of tectono-sedimentary interactions (*e.g.,* Shanmugam et al., 2017; Elisa et al., 2018; Zhang et al., 2022; Garde et al., 2023; Williams, 2023).

In the eastern Pacific, the convergent, subduction setting has formed a classic ocean-continent margin since at least latest Triassic times (Hervé, 1988; Ramos, 1999), offering a natural laboratory for studying seismic-tectonic linkages across the Meso-Cenozoic (Duan et al., 2017; Lu et al., 2023). However, geological records of pre-Quaternary earthquakes in this region are exceptionally sparse, restricting interpretations to recent seismic impacts (Dorbath et al., 1990; Benavente et al., 2012, 2021). Critically, seismite-based reconstructions of plate subduction history remain absent, hindering understanding of long-term tectonic evolution.

The present study addresses these knowledge gaps through an integrated analysis of Upper Jurassic seismites in the Chiclayo region of northern Peru. Stratigraphic measurements across three transects (Fig. 1) were conducted to characterize the geometry, lithology, and space and time distribution of deformation structures within the La Leche Formation. A thorough examination reveals the origins and defining characteristics of the La Leche seismites, whose formation patterns are crucial for determining the age of sedimentary strata, as well as for understanding the tectonic triggers and their implications for convergent plate dynamics.

Fig. 1. Geological sketch map of the Chiclayo area in northern Peru (modified from Jaimes et al., 2023). Gray circles: towns and cities. Fm: Formation. Gr: Group.

2. Geological setting

The Chiclayo region is located in the northern part of Peru, adjacent to the provinces of Lambayeque and Cajamarca, at the convergence of the Andean plains and the coastal Cordillera batholiths belt (Jaimes et al., 2023). Pervasive distribution of Mesozoic and Cenozoic volcanic and intrusive complexes is a distinctive characteristic of this region (Fig. 1).

The lower Paleozoic Salas Group, a metamorphic foundation, is unconformably overlain by the upper Permian-Lower Triassic molasse deposits of the Mitu Group. The Mesozoic stratigraphic succession in this region is comprised of several distinct formations, including the blocky limestone of the La Leche Formation (Upper Jurassic), the Oyotún Formation volcanics (Lower Cretaceous), the banded limestone of the Tinajones Formation (Lower Cretaceous), and the Goyllarisquizga Formation quartz sandstone (Lower Cretaceous) and its superjacent clasolites.

In the coastal margin of northern Peru, the Middle and Late Jurassic are represented by a suite of calc-alkaline volcanic and intrusive rocks (ca. 174-145 Ma) (Ingemmet, 2016; Jaimes et al., 2023). This igneous rock suite constitutes the primary body of the

Cordillera batholiths zone. During the Early Cretaceous (ca. 140-130 Ma), bimodal volcanic rocks developed in back-arc basins, such as the Pucará Basin (Duan et al., 2017; Alan et al., 2023). Subsequent to this initial phase, the region underwent intrusive activity represented by Upper Cretaceous (ca. 95-84 Ma) and Paleogene (ca. 52-28 Ma) stocks (Yao et al., 2024). The sedimentary strata of the coastal mountain range have experienced significant folding and faulting since, with pronounced block faulting (graben and horst) activity in the coastal Andean foreland plain, resulting in continuous surface uplift and subsidence.

The sedimentary strata of the coastal mountain range have functioned as essential ore-bearing wall rocks for skarn-type silver and lead-zinc deposits (Alan et al., 2023), while the Upper Cretaceous ignimbrites have acted as the primary ore-forming parent rocks for porphyry copper deposits. In the Cajamarca and Hualgayoc regions, epithermal gold±silver deposits exhibit a close association with Miocene volcanic activity.

3. Methods and materials

3.1 Survey and research methods

Initial interpretation of 1:100,000-scale geological data was conducted using satellite imagery to rapidly acquire regional-scale geological information. Subsequent field investigations in the Chiclayo area identified widespread brittle and soft-sediment deformation structures within the La Leche Formation. Three 1:10,000-scale geological sections were then measured in the La Leche, Chancay, and Zaña River valleys. Comprehensive evidence of geological structures, sedimentary environments, and facies was systematically documented. The stratigraphic sequences were subdivided with 1 m precision control, and samples of rock slices and adjacent beds were collected for age determination. A follow-up 1:50,000-scale regional survey in the Pampa del Chaparrí and Salas areas revealed spatial variations in stratigraphic sequence distribution and rock composition. Supplementary samples and field photographs were obtained. All laboratory analyses were performed at the Ministry of Natural Resources' East China Mineral Resources Supervision and Testing Center (China).

Fig. 2. Stratigraphic column and sedimentary environment of the La Leche Formation in the Chiclayo area.

3.2 Stratigraphic section materials

In the study region, the La Leche Formation (Pardo and Sanz, 1979) exhibits a complete stratigraphic sequence (Fig. 2). There is a distinct unconformity onto the underlying Mitu Group in the Pampa del Chaparrí area, while an unconformity is present beneath the overlying volcanic rocks of the Oyotún Formation in the La Leche area (Wilson, 1984). At the La Leche River section, from top to bottom, the stratigraphic bedsets within the La Leche Formation are (Fig. 2):

8. Gray-brown, thin-bedded siliceous banded limestone interbedded with gray-white fine-grained limestone. It includes liquefaction beaded gravels and liquefaction convolute lamination structures. Thickness: 40 m.
7. Light gray, medium to thin-bedded, fine-grained limestone and banded limestone, characterized by rhythmic bedding and bioturbation structures, along with signs of sliding and bending on the formation layers. Thickness: 50 m.
6. Grayish green, thick to medium-bedded dolomite limestone with uniform lithology and cyclic sequence. Some bioturbation structures are visible. Thickness: 32 m.

5. Dark gray, massive to thick-bedded, fine-grained limestone with calcarenite, which contains shell limestone and vermicular limestone. Thickness: 36 m.

4. Purple red, medium to thin-bedded calcareous quartz sandstone interbedded with gravel limestone, featuring locally fractured breccia and round gravel limestone. Thickness: 50 m.

3. Purple red, medium to thin-bedded gravel limestone interbedded with thin-bedded calcareous mudstone and bioclastic limestones. Brittle and soft-sediment deformation structures are present. Thickness: 70 m.

2. Green-gray, medium to thin-bedded calcarenite with calcareous mudstone, with internal microfaults, stepped faults, and water-escape structures visible. Thickness: 40 m.

1. Gray-green, thick to medium-bedded quartz sandstone interbedded with thin-bedded bioclastic limestones. Thick-bedded conglomerates at the bottom. Thickness: 40 m.

3.3 Regional stratigraphic comparison

The La Leche Formation exhibits a clear bipartite lithological division. Its upper portion comprises dark gray to grayish green, thick to medium-bedded fine-grained limestones, interbedded with medium to thin-bedded limestones, banded limestones, and bioclastic limestones. Diagnostic vermicular intraclasts are pervasive within these rocks. The lower portion consists of purple-red, thick to medium-bedded calcareous quartz sandstones, interstratified with gravelly limestones, calcarenites, and subordinate calcareous mudstones (Seilacher, 1984).

The lithology and thickness of the La Leche Formation exhibit significant variations. The Pampa del Chaparrí area is located at the periphery of a substantial dome structure, where profound strata are elevated and exposed, containing fossils such as corals, bivalves, and brachiopods (Wilson, 1984). The Salas region is notable for its thick-to-medium limestone beds. The La Leche and Oyotún formations appear sporadically along the Chancay River valley, from Patapo to Chongoyape and Guayabo, due to ongoing western uplift. The La Leche Formation features abundant brittle and soft-sediment deformation structures. The upper sequence includes vermicular limestones that exhibit a chaotic mixture of diverse animal fossils and syn-depositional deformation structures. The exposure of the La Leche Formation in the Zaña River valley is limited, consistently revealing thick-bedded gray limestone and grayish-green fine-grained limestone.

The thickness of the La Leche Formation varies from 250 to 700 m (Jaimes et al., 2023), with the La Leche River section measuring 358 m (Fig. 2). Within these sections, the concentrated brittle and soft-sediment deformation structures are identified in bedsets 2, 3, 4, 5, and 8 (Fig. 2). This distribution reflects controls by regional synsedimentary faulting, where differential positioning along the fault system resulted in varied lithology, thickness, and seismite development.

4. Results

Sediment deformation structures serve as crucial 'fingerprints' for interpreting the dynamics of ancient depositional environments and have long been central to the reconstruction of paleogeography, paleoclimate and abrupt geological events (Seilacher, 1969; Song, 1988; Van Loon, 2014; Brogi et al., 2018; Esther et al., 2022). These diverse structures, ranging from microscopic folds and fractures to large-scale convolutions and brecciation, faithfully document the various physicochemical processes that sediments experience during the post-depositional and early diagenetic stages. However, their complex formation mechanisms and morphological diversity present ongoing challenges for their accurate identification and classification by the

scientific community (Alsop and Marco, 2011; Lu et al., 2020; Walaa et al., 2022). In order to better elucidate the controlling factors behind these structures and their geological significance, an integrated classification scheme is adopted in this study based on genetic processes and degree of lithification (Qiao et al., 2009; Su et al., 2018; Berra, 2024). This classification scheme allows categorizing the deformation features observed in the La Leche Formation into three primary types: brittle deformation structures, soft-sediment deformation structures (SSDS), and turbidite structures. These are explained below.

4.1 Brittle deformation structures

Brittle deformation structures develop in consolidated or semi-consolidated sedimentary rocks under a tectonic regime characterized by tensile stress (*e.g.,* Liang et al., 2009; Lin et al., 2013). These structures include micro normal faults, fractured breccias, and Neptunian dikes.

Micro normal faults

Microfaults, characterized by a step-like, parallel lateral arrangement, with steep dip angles and minimal fault separation, are dispersed throughout thin rock beds and are typically dominated by extensional faults. In the La Leche Formation, these microfaults are found to be densely developed within the medium to thin-bedded calcarenites of bedset 2 in the La Leche River and Chancay River sections. They exhibit a stair-step parallel organization on the profile and form a planar network extension on the bed surface. The fault separation is typically minimal, of cm-scale (Fig. 3A), and the voids are predominantly infilled with subsequent calcite veins (Fig. 3B).

Fractured breccias

Fractured breccias are the result of *in situ* shattering of consolidated or partially consolidated sediments, which may be torn or sheared into brecciated and muddy gravel. These breccias are particularly concentrated within the medium to thin-bedded limestones and sandstones of bedsets 3 and 4 in the Chancay River section, respectively, where they have undergone multiple self-fragmentation processes to form autoclastic breccias. Some breccias incorporated gravel clasts, were further fragmented and subsequently restructured (Fig. 3C). Additionally, breccias may be superimposed on one another, resulting in imbricate thrusts or toe-like configurations, with distinct internal features indicative of a jigsaw assembly.

Neptunian dikes

Brittle fractures and Neptunian dikes have been identified in bedset 2 of the La Leche River section and bedsets 3 and 4 of the Chancay River section. The fractures exhibit an irregular orientation, extending in multiple directions (Fig. 3C), with widths ranging from 2-5 mm and an extent that can span several meters (Fig. 3D). The presence of multiple infillings and fracturing within the fissures indicates that they represent a class of synsedimentary microfractures. Neptunian dikes, defined as vein-like structures within limestone strata, exhibit widths of approximately 5 cm and extend beyond 200 cm. The dikes' walls are straight, and they are filled with limestones and carbonate micrite veins. These veins share similar compositional characteristics with the enclosing rock but contrast markedly in color and texture (Fig. 3D). This observation suggests that the rock experienced multiple episodes of self-fragmentation and subsequent infilling by liquefied clasts.

Fig. 3. Brittle deformation structures of the La Leche Formation in the Chancay River valley area (see figure 1 for location). **A.** Micro normal faults (yellow dotted lines) within the bed, arranged at a cm-scale, stepped lateral array. **B.** Microscopic normal faults within a limestone bed, filled

with calcite (parallel nicols). **C.** Fractured breccias and fracture structures, showing multiple filling and fracturing events. **D.** Brittle fractures and Neptunian dikes, exhibiting multiple processes of breccia rupturing and dike filling; order of occurrence is 1-2-3-4.

4.2 Soft-sediment deformation structures

SSDS are features that form syndepositionally or penecontemporaneously within water-saturated, unconsolidated to semi-consolidated sediments in response to transient forces. Their preservation potential is closely tied to lubrication effects of pore waters, sedimentation rates, and the intensity of triggering events. While various triggering mechanisms exist (e.g., gravity slumping, wave oscillations, volcanic tremors), seismic shaking is one of the causes in their development (Hilbert-Wolf et al., 2010; Alsop et al., 2011; Boukhedimi et al., 2017). Representative SSDS types include deformed laminations, slump structures, load-cast structures, and thixotropic diapir structures.

Deformed laminations

When soft, wet sedimentary beds are subjected to the combined effects of load pressure and pore water overpressure, the supporting framework of the water-saturated sediments becomes disrupted. This results in fluid overflow and the deformation of laminations. This phenomenon drives the vertical development of fine veins that promote upward drainage. Concurrently, horizontal evolution manifests as disc-shaped bedding and drainage channels, collectively termed water-escape structures and dish structures. These features have been observed in the medium to thin-bedded calcarenites of bedset 2 in the Chancay River section (Fig. 4A) and are also present in bedsets 2 and 8 of the La Leche River section, where distinct pore-water seepage channels are evident under microscopic examination (Fig. 4B).

Slump structures

Slump structures are distinguished by the presence of liquefaction beaded gravels and various small-scale slump folds, which are notable for sediment curling, compaction, and collapse. Furthermore, these structures exhibit enveloping or convolute bedding and sliding deformation within fine sandy and pelitic beds. (Fig. 4C, E, F). In the La Leche River section, prominent liquefaction beaded gravels (resembling boudin structures) and slump deformations are evident (Fig. 4D), representing the upper components of the sedimentary strata. Slump-structured beds constitute a well-developed sequence within bedset 8 of the La Leche River section (Fig. 4E), characterized by individual beds with thicknesses ranging from 10-30 cm and laminations 2-5 cm thick. The succession is characterized by the presence of fine-grained limestones and micritic limestones, interspersed with liquefaction beaded gravels, and siliceous banded limestones featuring convolute lamination (Fig. 4F), with a total thickness of 40 m. Subsequent to weathering, the slump folded sediments manifest a variety of rock patterns, thereby creating a distinctive natural landscape and serving as a unique identifier for the uppermost sedimentary strata of the La Leche Formation in the study area.

Fig. 4. SSDS of the La Leche Formation in the Chancay and La Leche river valley areas. **A.** Water-escape and dish structures within the lamination (Chancay area). **B.** Microscopic seepage channel through which pore water escaped laterally (parallel nicols; La Leche area). **C.** Folding deformation microfeatures formed by liquefaction processes (parallel nicols; La Leche area). **D.** Beaded gravels and boudin structures (La Leche area). **E.** Slump structures (Bedset 8, La Leche area). **F.** Weathered slump structures (La Leche area).

Load-cast structures

Load-cast structures are the result of the action of loading, which induces the liquefaction of mud-sand beds to penetrate or sink into adjacent sand layers. These features are identified in bedsets 3 and 4 of the Chancay River section (Fig. 5A) and bedset 2 of the La Leche River section (Fig. 5B), manifesting themselves as flame structures and mushroom-shaped sand bodies (Fig. 5C). Additionally, ball-and-pillow structures are present, where dismembered sand layers experience further fracturing, compaction, and rounding into pebbles or concentric spheres. The juxtaposition of rounded gravels arranges in sequence to create a stratified pseudo-conglomerate appearance (Fig. 5D).

Thixotropic diapir structures

They are distinguished by sediment deformation traces in the overlying and underlying surrounding rocks, resulting from the extrusion of liquefied sediment fluids, a process also referred to as extrusion techniques. These phenomena include thixotropic diapirs and Neptunian dikes. In bedset 2 of the La Leche River section, the size of these structures varies (Fig. 5E), being present even at the microscopic level (Fig. 5F). These structures are sometimes accompanied by carbonate micrite veins, formed concurrently due to material escaping during the extrusion process.

Fig. 5. SSDS of the La Leche Formation in the Chancay and La Leche River valley areas. **A.** Prospect of sedimentary sequence in the middle of the Chancay section. **B.** Interbedded sandy limestone and calcareous mudstone in the lower part of the La Leche section. **C.** Flame structures, mushroom-shaped sands, and self-fragmented breccias of load-cast structures (La Leche area). **D.** Juxtaposition of sand ball-and-pillow structure (Chancay area). **E.** Thixotropic diapir and flame structures (La Leche area). **F**. Microscopic thixotropic diapir structures (crossed nicols; La Leche area).

4.3 Turbidite structures

Turbidites are particularly well-developed in steep-gradient settings such as fault scarps, intracontinental rift basins, passive continental margins, and continental slopes (*e.g.,* Tappin et al., 2014; Du et al., 2020). A notable example is the co-occurrence of autoclastic breccias alongside turbidites that encompass sandy bodies (Chen et al., 2021), where incomplete Bouma sequences have been identified. These deposits are present in bedset 8 of the La Leche River section and bedset 5 of the Pampa del Chaparrí area, exhibiting well-developed Bouma sequences (Fig. 6A, B) and locally accumulated sand bodies with graded bedding (Fig. 6C). In localized areas, basal scour structures can be observed within the rock layer (Fig. 6D).

Thick-bedded calcarenite in the lower part of the turbidite sequence in bedset 5 of the Chancay and Pampa del Chaparrí areas is intercalated with multiple layers of thick vermicular limestone. The matrix of the vermicular limestone is made up of fine-grained limestone, while the vermiculation itself is made up of allochemical limestone. The vermiform structures measure approximately 10–30 cm in length and 2–5 cm in width. They exhibit worm-like morphology, plastic deformation, subtle preferred orientation, rounded edges, and sharp contacts with the matrix (Fig. 6E). These features are the result of syndepositional deformation processes affecting unconsolidated turbiditic sediments (Owen, 1987; Henry et al., 2019).

Fig. 6. Turbidite structures of the La Leche Formation in the Chiclayo area. **A.** Turbiditic sedimentary sequence, general view (Pampa del Chaparrí area). **B.** Incomplete Bouma sequence (La Leche area); Ta, Tb, and Tc being the depositional units within it. **C.** Graded bedding in sandstone

(Pampa del Chaparrí area). **D.** Basal scour structures (Pampa del Chaparrí area). **E.** Vermicular limestone (Chancay area).

4.4 Lithofacies and paleogeography

The region experienced prolonged exposure and uplift from the Late Triassic to the Early-Middle Jurassic. Sedimentation resumed in the Late Jurassic, transitioning from littoral to shallow marine environments across the continental shelf (Kevin et al., 1992; Li et al., 2016). Analysis of the sedimentary facies of the La Leche Formation confirms these previous interpretations but reveals a far more complex paleogeographic evolution.

From bottom to top (Fig. 2), bedset 1 comprises conglomerates and well-rounded, cross-bedded quartz sandstones, indicative of a littoral clastic beach or sand dune environment. Bedsets 2 and 3 form a cyclic sequence of interbedded limestone and medium to thin-bedded calcareous mudstone with parallel and cross-bedding. The presence of bioclastic limestone suggests deposition in a shallow marine-littoral environment. Bedset 4 is characterized by a significant influx of continental margin clastics with minor supralittoral deposits, representing a littoral facies with enhanced terrestrial input. Bedsets 5 and 6 are dominated by thick, lithologically uniform limestones exhibiting massive bedding and bioturbation features, indicative of a transition to a shallow marine shelf environment on a restricted carbonate platform, with localized tidal channels that may contain turbidite fills. Bedset 7 displays low-energy sedimentation features characteristic of the shallow marine-subtidal zone, with rhythmic and cross-bedding structures attributed to tidal currents. Finally, bedset 8 consists of interbedded siliceous banded limestones and fine-grained limestones, characterized by abundant convolute bedding structures and turbiditic deposits, indicative of a continental shelf to shallow marine depositional setting and reflecting sedimentation influenced by turbulent seawater incursion.

Taking into account the spatial relationships between the La Leche Formation, the overlying Oyotún Formation and the regional stratigraphy, it is possible to interpret these units as components of the Mesozoic Central Andean island arc system. Specifically, the La Leche Formation accumulated within a Late Jurassic initial back-arc basin (Jaimes et al., 2023). The sedimentary sequence of the basin exhibits remarkable lithological diversity, characterized by multiple sets of composite depositional systems formed through the alternation of traction currents and gravity flows. The presence of deep-water facies associations, such as olistostromes and turbidites, reveals that slope instability events were triggered by relatively frequent tectonic activity. This resulted in elevated sedimentation rates, reduced permeability, and a decreased consolidation coefficient (Li et al., 2025), which kept the sediments under-consolidated. Rapidly stacked and chaotically distributed fossil communities within bioclastic limestones corroborate the instantaneous supply of provenance and the rapid burial processes that followed individual tectonic events. Extensive development of zonally distributed and densely occurring sediment deformation structures across the the La Leche, Chancay and Zaña river valleys demonstrates the effects of localized stress concentration induced by tectonic activity. The structural architecture of this back-arc basin, particularly its fault-bounded segments and slope settings, created favorable conditions for the widespread development of seismites during seismic events (Montenat et al., 2007).

5. Discussion

5.1 Seismites and sedimentary sequences

Discrimination of seismites

The identification of seismites relies on detecting diverse sediment deformation structures within the stratigraphy (*e.g.,* Seilacher,

1969; Hilbert-Wolf et al., 2010; Boukhedimi et al., 2017; Du et al., 2017). However, due to the varied origins of such structures, multiple lines of evidence are required to confirm them (*e.g.,* Owen et al., 2010; Shanmugam et al., 2017; Alsop et al., 2019). Differentiating seismogenic deformation from structures formed by other processes remains a challenging and controversial endeavor (Qiao et al., 2009; Su et al., 2018; Berra, 2024).

The La Leche Formation exhibits an abundance of brittle, soft-sediment and turbidite structures. Such features do not typically form in normal subaqueous environments; rather, they are the result of disturbances caused by abrupt geological events (Xing et al., 2016; Dilce et al., 2017). Large-scale soft-sediment deformation structures, in particular, indicate the plastic response of unconsolidated sediments under rapid loading conditions, with seismic activity being a critical contributor. Stepped microfault systems, classified as brittle deformation structures, and associated Neptunian dike structures, observed across multiple stratigraphic levels, directly reflect the instantaneous shear forces acting on loosely packed sedimentary layers during tectonic processes. The primary source of this instantaneous shear is seismic activity, which records the fracturing of rock layers induced by seismic wave propagation. Consequently, these structures serve as critical paleoseismic indicators within the stratigraphic record (Seilacher, 1969; Du et al., 2017).

The upper sequence of the La Leche Formation comprises turbidites formed in a shallow-water littoral environment. The significant facies shifts and sharp lithological boundaries within these deposits suggest that background sedimentation was episodically disrupted, likely by sudden events such as earthquakes. Frequent seismic shaking would resuspend seafloor sediments, which would then be redeposited as graded units or turbidites (Feng, 2017; Chen et al., 2021). This process could also trigger landslides or cliff collapses, or generate turbidity currents and seismites. The cyclical accumulation and release of tectonic stress could have provided the dynamic mechanism for recurring seismic activity. Based on an integrated analysis of these features, the sedimentary deformation structures within the La Leche Formation are interpreted as seismites.

5.1.2 Seismite sedimentary sequences

Seismite sedimentary sequences comprise vertically stacked sedimentary units deposited or remobilized during a seismic event and its secondary consequences (e.g., tsunamis, turbidity currents). The analysis of these sequences is fundamental for deciphering the origins of brittle and soft-sediment deformation structures (Moretti et al., 2014; Van Loon, 2014; Du et al., 2017). Tectonic and depositional settings exert primary control over the diversity of seismite sedimentary sequences (He and Zhang, 2002). Based on their dominant triggering and depositional processes, they are classified into: seismite sedimentary sequences (*sensu stricto*), seismo-turbidite sedimentary sequences, seismo-tsunamite sedimentary sequences, and composite seismite sedimentary sequences. The temporal framework for establishing a seismite sedimentary sequence is defined relative to the causative earthquake; that is, pre-seismic phase, mainshock phase, aftershock phase, and post-seismic phase. Sediment units within the sequence are further distinguished by provenance as autochthonous or allochthonous (Du et al., 2016; Bai et al., 2021; Chen et al., 2021).

Eight seismite units are identified within the La Leche Formation (Fig. 7): A. Background sediment (unaffected); B. Seismic fractured breccia; C. Stepped faults layer; D. Load-cast structures and beaded gravels; E. Neptunian dikes and microfaults; F. Seismically folded layer and liquefied convolute lamination; G. Homogenized liquefaction layer; H. Seismo-turbidite and tsunamite. This vertical sequence reflects the dual-layer depositional model typical of seismites (Jiang et al., 2020), comprising: autochthonous units (B–G), which are in-situ deformed sediments, and an allochthonous unit (H), which consists of reworked and transported deposits. The seismite sedimentary sequence manifests through various combinations of these units, with individual thicknesses ranging from several meters to over 15 m and grouped into five prominent seismite horizons (bedsets 2, 3, 4, 5, and 8) within the La

Leche River section.

Deformation structure analysis provides key constraints on seismic intensity. Sediment liquefaction initiation requires an intensity of at least V–VI (Berra et al., 2011). The formation of specific features, such as Neptunian dikes, liquefaction breccias and beaded gravels, indicates intensities typically within the VI–VII range (Obermeier, 1996; Qiao et al., 2009). The presence of these five seismite bedsets demonstrates that multiple seismic events with an intensity of at least VI occurred during the deposition of the La Leche Formation.

Fig. 7. Seismic sedimentary sequence of the La Leche Formation in the Chiclayo area.

5.2 Discussion on the era of La Leche Formation

The age of the La Leche Formation in Peru remains poorly constrained. Fossil assemblages (corals, bivalves, brachiopods) from this formation correlate with those of the lower part of the eastern Pucará Group (Jaillard et al., 1999), previously interpreted as Late Triassic to Early Jurassic (Wilson, 1984). However, recent LA-ICP-MS U-Pb zircon dating of dacitic rocks at the top of the Pucará Group yields a precise age of 131.3 ± 1.5 Ma, confirming an Early Cretaceous mature back-arc basin setting for this unit. Furthermore, LA-ICP-MS U-Pb zircon ages of volcanic rocks from the overlying Oyotún Formation range from 131.0 to 139.7 Ma (Duan et al., 2017; Jaimes et al., 2018). This evidence revises the age of the Oyotún Formation from Middle-Late Jurassic to Early Cretaceous, identifying it as part of an Early Cretaceous volcanic arc.

The Chocolate, Río Grande, and Oyotún formations, as well as the Pucará Group and other volcanic units in the Western Cordillera of Peru unconformably overlie the upper Permian-Lower Triassic Mitu Group. These units were traditionally assigned a Late Triassic to Late Jurassic age (Ingemmet, 2016); however, collaborative research between the China Geological Survey and the Instituto Geológico Minero y Metalúrgico of Peru over the past decade reviewed the age of this entire volcano-sedimentary package to Late Jurassic–Early Cretaceous (Jaimes et al., 2018, 2023). This revised chronology indicates that significant tectonic and volcanic activity in the Western Cordillera commenced primarily in the Late Jurassic. In consequence, the La Leche Formation is assigned to the Late Jurassic, representing initial back-arc basin sedimentation along the proto-Western Cordillera. The seismites and sedimentary sequences of this formation were part of a littoral-shallow marine shelf within a continental-margin back-arc basin.

5.3 Earthquake triggering mechanisms

During the Late Jurassic, the proto-Farallon plate, which was subducting beneath western South America, underwent rollback (Hervé et al., 2014; Wu et al., 2015; Duan et al., 2017; Bian et al., 2024), forming a strongly extensional tectonic environment (Moretti et al., 2007; Owen et al., 2010; Morsilli et al., 2020; Nirmalya et al., 2022). Intense seismic activity related to this new geodynamic configuration is evidenced through the brittle and soft-sediment deformation structures identified within the La Leche Formation, which are unequivocally classified as seismites. Global studies of seismites indicate that they develop preferentially in extensional environments dominated by active faulting, particularly normal and transtensional faults (Odonne et al., 2011; Balázs and Brian, 2016; Alsop et al., 2019; Chen et al., 2020). Modern seismicity patterns in Peru corroborate this, revealing intense activity localized within an extensional environment driven by plate subduction, chiefly along the upper portions of major subduction thrust interfaces and deep crustal faults bordering back-arc basins (Benavente et al., 2012, 2021).

The spatial location of the La Leche seismites aligns with the inferred paleo-leading edge of the Coastal Cordillera, extending

north-west along the proto-continental margin and adjacent coastal plains. This distribution intersects with major paleo-drainage systems (*e.g.,* the Salas, La Leche, Chancay, and Zaña valleys), effectively outlining the boundary of the Late Jurassic back-arc basin (coastal plain). A series of synsedimentary normal faults developed along the western flank of the nascent Coastal Cordillera, creating an extensional, seismically active zone. Earthquake-driven co-seismic collapses along these basin-margin faults, coupled with gravity-driven resedimentation within the basin, are the primary mechanisms behind the observed seismites (He et al., 2021; Abdel Fattah et al., 2023; Gupta et al., 2024).

The sedimentary environment and triggering mechanisms of the La Leche seismites support the interpretation that the Mesozoic Andean orogeny involved complex, non-steady-state subduction rather than a simple, continuous ocean-continent process (Wang et al., 2022; Zeng et al., 2023). This intricate process involved episodic subduction advance, slab tearing and potential lower mantle interactions (Walter et al., 2018; Chen et al., 2019), and induced significant upper-plate extension. The resulting seismogenic fault activity generated the regional earthquakes recorded in the La Leche Formation stratigraphy.

6. Conclusions

1. The La Leche Formation in the Chiclayo area of northern Peru represents a Late Jurassic coastal to shallow marine carbonate succession that was deposited in a littoral to shallow shelf environment. It is characterized by abundant bioclastic material, a significant lateral extent and well-defined environmental facies relationships.
2. Within the La Leche Formation, the presence of brittle and soft-sediment deformation structures, as well as turbiditic sequences, collectively identify them as seismites. These features record at least five seismic events of intensities VI or higher.
3. The La Leche Formation was deposited within an initial back-arc basin, formed due to the subduction of the paleo-Farallon tectonic plate beneath South America. This seismic sequence corresponds to the limestone interval of the lower Pucará Group and can be firmly dated to the Late Jurassic.
4. Seismite formation was induced by synsedimentary fault activity along the boundary between the western coastal mountains and the coastal plain.

This article celebrates and reviews Professor Francisco Hervé's six-decade contribution to the study of geological evolution. His pioneering subduction-accretionary wedge model for late Paleozoic tectonics in southern Chile revealed the early stages of Andean orogeny and clarified pre-Mesozoic crustal dynamics. The application of detrital zircon U-Pb dating that he developed to trace provenance and tectonic affinities in metamorphic complexes is still a cornerstone methodology in terrane analysis today. Many Chinese people remain deeply grateful for his invaluable support in hosting the 30th International Geological Congress, an event that significantly advanced global geoscience collaboration. As authors who have greatly benefited from his outstanding work, we extend our heartfelt congratulations with the traditional blessing:

(May your life endure like the southern mountains' ancient pines, evergreen through time; your wisdom spans continents, like ivy eternally thriving in the pursuit of knowledge).

Acknowledgments

We sincerely appreciate the support from the Nanjing Center, China Geological Survey (CGS) and the Instituto Geológico Minero y Metalúrgico (Ingemmet) for providing us with a research base and technical support for our work. We are grateful to Dr. X. Guangfu, Prof. X. Mincheng, Dr. W. Tiangang, and Dr. Z. Xuehui of CGS for discussing the relevant problems and difficulties we encountered during the field investigation and writing process. We would like to express our special gratitude to Prof. Dr. H. Weihong of the China University of Geosciences (CUG) and to Prof. Dr. M. Spiske, Dr. R. Pankhurst, and one anonymous reviewer for their invaluable technical guidance. Their support was a great source of inspiration in completing this article. This work was funded by the Central Financial Geological Survey Project of the China Geological Survey (DD20230129 and DD20230051).

References

Abdel Fattah, M.M., Abu Sharib, A.S.A.A. 2023. Liquefaction-induced structures, Hammam Faroun Block, Gulf of Suez rift, Egypt: possible rift-related Neogene seismites. International Journal of Earth Sciences, 112(3): 1-19. https://doi.org/10.1007/s00531-023-02289-3

Alan, S., Guo, W.M., Chen, N.A., Luis, C., Shoji, K. 2023. Geochronologically constrained life cycles of telescoped porphyry-epithermal systems at the La Arena district, Northern Peru. Ore Geology Reviews, 155: 105375. DOI: 10.1016/j.oregeorev.2023.105375.

Alsop, G.I., Marco, S. 2011. Soft-sediment deformation within seismogenic slumps of the Dead Sea Basin. Journal of Structural Geology, 33(4):433-457. DOI: 10.1016/j.jsg.2011.02.003.

Alsop, G.I., Weinberger, R., Marco, S., Levi T. 2019. Identifying soft-sediment deformation in rocks. Journal of Structural Geology, 125: 248-255. DOI: /10.1016/j.jsg.2017.09.001.

Bai, P.R., Ma, D.S., Xiong, X.G., Zeng, Y.R. 2021. Discovery and significance of seismites in Carboniferous Nuocuo Formation in Jiuzila area, Dangxiong, Tibet. Journal of Stratigraphy, 45(1): 49-57. DOI: 10.19839/j.cnki.dcxzz.2021.0009.

Balázs, T., Brian, R.P. 2016. Sedimentary record of seismic events in the Eocene Green River Formation and its implications for regional tectonics on lake evolution (Bridger Basin, Wyoming). Sedimentary Geology, 344: 175-204. DOI: 10.1016/j.sedgeo.2016.02.003.

Benavente, C., Fabrizio, D., Spiske, M., Audin, L. 2012. Seismites and paleotsunamis deposits, assessing for paleoseismicity in Peru[C]// Pérez-López, R, Silva, P.G, Rodríguez, M.A. Proceedings 3rd INQUA-IGPC 567 International Workshop on Earthquake Geology, Palaeoseismology and Archaeoseismology, Morelia, Mexico, 3: 21-24.

Benavente, C., Wimpenny, S., Rosel, L., Robert, X., Palomino, A., Audin, L., Aguirre, E., García, B. 2021. Paleoseismic Evidence of an Mw 7 Pre-Hispanic Earthquake in the Peruvian Forearc. Tectonics, 2021(6). DOI: 10.1029/2020TC006479.

Berra, F. and Felletti, F. 2011. Syndepositional tectonics recorded by soft-sediment deformation and liquefaction structures (continental Lower Permian sediments, Southern Alps, Northern Italy): Stratigraphic significance. Sedimentary Geology, 235:

249-263. DOI: 10.1016/j.sedgeo.2010.08.006.

Berra, F. 2024. Soft-sediment deformation structures and Neptunian dykes across a carbonate system: Evidence for an earthquake-related origin (Norian, Dolomia Principale, Southern Alps, Italy). Sedimentology, 71: 827-849. DOI: 10.1111/sed.13154.

Bian, H. D., Liu, Z. L., Feng, S. M., Wang, Y. 2024. Tectonic shortening at plate spreading centers. East China Geology, 45(4): 381-386.

Boukhedimi, M.A., Louni-Hacini, A., Bouhadad, Y., Ritz, J.F., Machane, D., Benhamouche, A., Bourenane, H. 2017. Evidence of seismites in coastal Quaternary deposits of western Oranie (Northwestern Algeria). Journal of Seismology, 21(3): 539-549. DOI: 10.1007/s10950-016-9616-2.

Brogi, A., Capezzuoli, E., Moretti, M., Olvera-Garci´a, E., Matera, P.F., Garduno-Monroy, V.H., Mancini, A. 2018. Earthquake-triggered soft-sediment deformation structures (seismites) in travertine deposits. Tectonophysics, 745: 349-365. DOI: 10.1016/j.tecto.2018.08.021.

Buchner, E., Volker, J.S., Schmieder, M. 2020. New discovery of two seismites horizons challenges the Ries-Steinheim double-impact theory. Scientific Reports, 10(1): 22143. DOI: 10.1038/s41598-020-79032-4

Chen, A., Zhong, Y., Ogg, J.G., Van Loon, A.J.T., Chen, H., Yang, S., Liu, L., Xu, S. 2020. Traces of the Triassic collision between the North and South China blocks in the form of seismites and other event layers. Journal of Geodynamics, 136: 101720. DOI: 10.1016/j.jog.2020.101720

Chen, G.Y., Liu, G.C., Ma, J.H., Chen, K., Sun, B.D., Yan, X., Sun, P., He, Z.R. 2021. The Late Triassic seismic soft sedimentary, deformation and its event significance in the west margin of Chuxiong Basin. Geological Bulletin of China, 40(7): 1011-1023.

Chen, Y.W., Wu, J., John, S. 2019. Southward propagation of Nazca subduction along the Andes. Nature, 565(7740): 441-447.

Cheng, L., Li, G.T., Wu, H., Yu, J.Q., Su, G. 2020. A Preliminary Study of Paleo-earthquake in the Majiacun-Daju Section of Zhongdian-Daju Fault, Yunnan Province. Earthquake Research in China, 36(2): 211-220.

Cita, M.B., Lucchi, F.R. 1984. Special Issue-Seismicity and Sedimentation Preface. Marine Geology, 55(1/2): 7-10. DOI: 10.1016/0025-3227(84)90128-2.

Dilce, F.R., Fabio, C.A., Marcio, M.V. 2017. A tectonically-triggered late Holocene seismite in the southern Amazonian lowlands, Brazil. Sedimentary Geology, 358: 70-83. DOI: 10.1016/j.sedgeo.2017.07.003

Dorbath, L., Cisternas, A., Dorbath, C. 1990. Assessment of the size of large and great historical earthquakes of Peru. Bulletin of the Seismological Society of America 80 (3): 551-576. DOI: 10.1016/0040-1951(90)90455-H.

Du, F.P., Wang, J.Q., Niu, J.Q., Tan, F.R., Yang, C., Yan, M.M. 2016. Characteristics and Its Significance of Soft Sedimentary Deformations of the Upper Triassic Bagong Formation in Southeastern Qiangtang Block. Journal of Jilin University (Earth Science Edition) , 46(3) : 661-670. DOI: 10.13278 /j.cnki.jjuese.201603104.

Du, Y.S., Yu, W.C. 2017. Earthquake-caused and non-earthquake-caused soft-sediment deformations. Journal of Palaeogeography, 19(1): 65-72. DOI: 10.7605/gdlxb.2017.01.005.

Du, Y.S., Han, X. 2000. Seismo-deposition and seismites. Advance in Earth Sciences, 15(4): 389-394.

Duan, Z., Guo, W.M., Zeng, Y., Liu, J.A., Igor, A.F., Leyla, G.M. 2017. Sequence, age and geochemistry of volcanic rocks of the Early Cretaceous Oyotún Formation in northwestern Peru: Revelation for the details of paleo-Farallon subduction. Geological Bulletin of China, 36(12): 2243-2263.

Elisa, K., Mordechai, S., Shmuel, M. 2018. Integrated Paleoseismic Chronology of the Last Glacial Lake Lisan: From Lake Margin

Seismites to Deep-Lake Mass Transport Deposits. Journal of Geophysical Research. Solid Earth, 123(4): 2806-2824. DOI: 10.1002/2017JB014117

Esther, M.S.M., Pablo, J.R.A. 2022. Seismites in Miocene gypsum microbialites: Multiproxy tools for paleoenvironmental reconstruction of saline lakes. Sedimentary Geology, 439:106219. DOI: 10.1016/j.sedgeo.2022.106219.

Feng, Z.Z. 2017. Preface of the Chinese version of "The seismite problem". Journal of Palaeogeography, 19(1): 13-17. DOI：10.1016/j.jop.2016.10.003.

Garde, A.A., Johansson, L., Keulen, N., Schreiber, A., Wirth, R. 2023. Zircon Microstructures in Large, Deeply Eroded Impact Structures and Terrestrial Seismites. Journal of Petrology, 64(11): 1-23. DOI: 10.1093/petrology/egad079.

Gong, Y.M. 1988. Tempestite, seismite and tsunamite: A discussion of several sedimentological terms. Geological Review, 34(5): 481-482.

Gupta, A., Verma, A.K., Yadav, B. 2024. Seismites as an indicator of active faulting along the Moradabad Fault: A further study on neotectonics in the Indo-Gangetic plains. Journal of Earth System Science, 133(1): 21. DOI: 10.1007/s12040-023-02227-6.

He, B.Z., Jiao, C.L., Cai, Z.H., Liu, R.H., Joseph, G.M., Yun, X.R., Wang, T.Y., Chen, W.W., Yu, Z.Y., Li, J.C., Peng, S.T., Hao, G.M., Guo, X.P., Qiao, X.F. 2021. Soft-sediment deformation structures (SSDS) in the Ediacaran and lower Cambrian succession of the aksu area, NW Tarim Basin, and their implications. Palaeogeography Palaeoclimatology Palaeoecology, 567(3): 110237. DOI: 10.1016/j.palaeo.2021.110237.

He, W.H., Zhang, K.X. 2002. Research on Outcrop Sequence Stratigraphy of Permian in Middle-Lower Yangtze Region. Journal of China University of Geosciences, 13(002): 192-202.

Henry, W. P., Venkatarathnam, K., Liu, H.Q. 2019. An Overview of Deep-water Turbidite Deposition. Acta Sedimentologica Sinca, 37(5):879-903. DOI: /10.14027/j.issn.1000-0550.2019.049.

Ingemmet. 2016. Mapa Geológico del Perú. Scale 1: 1 000 000. Versión digital estandarizada[M/CD]. Instituto Geológico Minero y Metalúrgico. Lima. https: //repositorio.ingemmet.gob.pe/handle/20.500.12544/3859.

Hervé, F. 1988. Late Paleozoic subduction and accretion in Southern Chile. Andean Geology, 15(1): 141-163. DOI: 10.18814/epiiugs/1988/v11i3/005.

Hervé, F. Christopher & Calderón., Mauricio & Mpodozis., Constantino. 2014. Early Permian to Late Triassic batholiths of the Chilean Frontal Cordillera (28°–31°S): SHRIMP U–Pb zircon ages and Lu–Hf and O isotope systematics. Lithos. s 184–187. 436-446. DOI: 10.1016/j.lithos.2013.10.018.

Hilbert-Wolf, H.L., Simpson, E.L., Simpson, W.S., Tindall, S.E., Wizevich, M.C. 2010. Insights into syndepositional fault movement in a foreland basin., trends in seismites of the Upper Cretaceous, Wahweap Formation, Kaiparowits Basin, Utah, USA. Basin Research, 21(6):856-871. DOI: 10.1111/j.1365-2117.2009.00398.x.

Jaillard, E., Laubacher, G., Bengtson, P., Annie, D., Luc, B. 1999. Stratigraphy and evolution of the Cretaceous forearc Celica-Lancones Basin of Southwestern Ecuador. Journal of South American Earth Sciences, 12: 51-68. DOI: 10.1016/S0895-9811(99)00006-1.

Jaimes, S.F., Guo, W.M., Cereceda, Q. 2023. Geología de los cuadrángulos de Chiclayo (hojas 14d1, 14d2, 14d3, 14d4) y Chongoyape (14e1, 14e2, 14e3, 14e4). INGEMMET, Boletín[R]. Serie L: Actualización Carta Geológica Nacional (Escala 1: 50 000), 51: 1-137, 8 mapas.

Jaimes, S.F., Guo, W.M., Eber, C. 2018. Nuevas interpretaciones en el emplazamiento de los volcánicos de la formación Oyotún y

su relación con la metalogenia[C]// Congreso Peruano de Geología, 19, Lima, Resúmenes ampliados. Lima: Sociedad Geológica del Perú, 509-512.

Kevin, A.L., David, R.G. 1992. Fluvial, coastal, nearshore, and shelf deposition in the Upper Proterozoic (?) to Lower Cambrian Addy Quartzite, Northeastern Washington. Sedimentary Geology, 77(1-2): 15-35. DOI: 10.1016/0037-0738(92)90101-V.

Levi, T., Weinberger, R., Alsop, G.I., Marco, S. 2018. Characterizing seismites with anisotropy of magnetic susceptibility. Geology, 46(9): 827-830. DOI: 10.1130/G45120.1.

Li, M.Z., Sun, M.J., Shan, Z., Hu, M.Y., Wu, S.F., Cai, H., Jiang, M.J. 2025. Under-consolidation characteristics of an offshore marine clay from Yellow Sea, China,Applied Ocean Research, 159,104591. DOI: 10.1016/j.apor.2025.104591.

Li, Y.Q., He, D.F., Chen, L.B., Mei, Q.H., Li, C.X., Zhang, L. 2016. Cretaceous sedimentary basins in Sichuan, SW China: Restoration of tectonic and depositional environments. Cretaceous Research, 57: 50-65. DOI: 10.1016/j.cretres.2015.07.013.Liang, D.Y., Nie, Z.T., Song, Z.M., Zhao, C.H., Chen, K.G., Gong, H.B. 2009. Seismic-tsunami sequence and its geological features of Mesoproterozoic Wumishan Formation in Fangshan Global Geopark, Beijing, China: a case study on Yesanpo scenic district. Geological Bulletin of China, 28(1): 30-37. DOI: 10.1016/S1874-8651(10)60080-4

Lin, S.G., Zheng, R.C., Liu, M.C., Wang, C.Y. 2013. Formation Mechanism and Significance of Continental Clastic Seismites . Natural Gas Geoscience, 24(1): 78-84.

Lu, Y., Wetzler, N., Waldmann, N. 2020. A 220,000-year-long continuous large earthquake record on a slow-slipping plate boundary. Science Advances. 6(48): eaba4170.DOI:10.1126/sciadv.aba4170.

Lu, F., Zhang, Y., Zhang, X.H., Mo, Z.F., Lu, J.S., Wu, B. 2023. Zircon U-Pb geochronology, geochemical characteristics and geological significance of the Chakeng granite porphyry, northeast Jiangxi Province. East China Geology, 44(01): 39-50.

Max, O.K., David, J.L., Vicki, G.M., Chaneva, J., Johnston, R., Villamor, P., Ilanko, T., Melchert, R.A., Orense, R.P., Loame, R.C., Ross, N. 2023. Seismically-induced down-sagging structures in tephra layers (tephra-seismites) preserved in lakes since 17.5 cal ka, Hamilton lowlands, New Zealand. Sedimentary Geology, 445: 106327. DOI: 10.1016/j.sedgeo.2022.106327

Montenat, C., Barrier, P., Ottd'Estevou, P., Christian, H. 2007. Seismites: An attempt at critical analysis and classification. Sedimentary Geology, 196(1): 5-30. DOI: 10.1016/j.sedgeo.2006.08.004

Moretti, M., Sabato, L. 2007. Recognition of trigger mechanisms for soft-sediment deformation in the Pleistocene lacustrine deposits of the Sant'Arcangelo Basin (Southern Italy): Seismic shock vs. overloading. Sedimentary Geology, 196(1-4): 31-45. DOI: 10.1016/j.sedgeo.2006.05.012.

Moretti, M., Loon, A.J.V. 2014. Restrictions to the application of diagnostic criteria for recognizing ancient seismites. Journal of Palaeogeography, 3(2): 162-173.

Morsilli, M., Bucci, M.G., Gliozzi, E., Lisco, S., Moretti, M. 2020. Sedimentary features influencing the occurrence and spatial variability of seismites (late Messinian, Gargano Promontory, southern Italy). Sedimentary Geology, 401: 105628. DOI: 10.1016/j.sedgeo.2020.105628.

Nirmalya, C., Malay, M., Anindya, S. 2022. A single extensional, diffuse, ductile fault zone in the Goriganga section, western Himalaya: Part of the upper South Tibetan Detachment System? . Tectonophysics, 841: 229561. DOI: 10.1016/j.tecto.2022.229561.

Obermeier, S.F. 1996. Use of liquefaction-induced features for paleoseismic analysis - An overview of how seismic liquefaction features can be distinguished from other features and how their regional distribution and properties of source sediment can be

used to infer the location and strength of Holocene paleo-earthquakes. Engineering Geology, 44(1-4): 1-76. DOI: 10.1016/s0013-7952(96)00040-3.

Odonne, F., Callot, P., Debroas, E.J., Sempere, T., Hoareau, G., Maillard, A. 2011. Soft-sediment deformation from submarine sliding: Favourable conditions and triggering mechanisms in examples from the Eocene Sobrarbe delta (Ainsa, Spanish Pyrenees) and the mid-Cretaceous Ayabacas Formation (Andes of Peru). Sedimentary Geology, 235(3): 234-248. DOI: 10.1016/j.sedgeo.2010.09.013

Owen, E.W. 1987. Tectonic control of resedimented conglomerates and associated sedimentary facies. Geological Society of America Bulletin, 98(5):617-630.

Owen, G., Moretti, M. 2011. Identifying triggers for liquefaction-induced soft-sediment deformation in sands. Sedimentary Geology, 235(4): 141-147. DOI:10.1016/j.sedgeo.2010.10.003.

Pardo, A., Sanz, V. 1979. Estratigrafía el curso medio del Río La Leche, Departamento de Lambayeque. Boletín Sociedad Geológica del Perú, 60: 251-266.

Qiao, X.F., Li, H.B. 2009. Effect of earthquake and ancient earthquake on sediments. Journal of Palaeogeography (Chinese Edition), 11(6): 593-610. DOI: 10.7605/gdlxb.2009.06.001.

Ramos, V.A. 1999. Plate tectonic setting of the Andean Cordillera. Episodes, 22: 183-190. DOI: 10.18814/epiiugs /1999/v22i3/005.

Seilacher, A. 1969. Fault-granded beds interpreted as seismites. Sedimentology, 13(1-2): 155-159.

Seilacher, A. 1984. Sedimentary structures tentatively attributed to seismicevents. Marine Geology, 55(1 /2): 1-12.

Serkan, Ü., Erman, Ö., Selçuk, A.S. 2019. Seismites as an indicator for determination of earthquake recurrence interval: A case study from Erciş Fault (Eastern Anatolia-Turkey) . Tectonophysics, 766: 167-178. DOI: 10.1016/j.tecto.2019.06.010.

Shanmugam, G. 2016. The seismite problem. Journal of Palaeogeography, 5(4): 318-362. DOI: 10.1016/j.jop.2016.06.002.

Shanmugam, G., Feng, Z.Z., Liu, M. 2017. The seismite problem. Journal of Palaeogeography, 19(1): 19-46. DOI: 10.7605/gdlxb.2017.01.004

Song, T.R. 1988. A possible suit of seismo-tsunami sequence in Precambrian carbo nate rock stratum in Shisanling in Beijing. Chinese Science Bulletin, 38(8): 609-611.

Su, D.C., Qiao, X.F. 2018. Discussion on the Term of Seismite and Its Chinese Translations. China Terminology, 20(6): 39-43. DOI: 10.3969/j.issn.1673-8578.2018.06.007.

Tappin, D.R., Grilli, S.T., Harris, J.C., Geller, R.J., Masterlark, T., Kirby, J.T., Shi, F., Ma, G. 2014. Thingbaijam, K.K.S., Mai, P.M. 2014. Did a submarine landslide contribute to the 2011 Tohoku tsunami?. Marine Geology, 357, 344-361. DOI: 10.1016/J.MARGEO.2014.09.043.

Van Loon, A.J. 2014. The life cycle of seismite research. Geologos, 20: 61-66. DOI: 10.2478/LOGOS-2014-0005

Walaa, A.H., Ezzat, A.A., Rashad, S., Mohamed, A.M., Mostafa, R.A. 2022. Evidence for Upper Cretaceous seismites in the Abu Tartur area, Western Desert, Egypt. Journal of African Earth Sciences, 187: 104452. DOI: 10.1016/j.jafrearsci.2022.104452

Walter, C., Guo, W.M., Mirian, M. 2018. Geocronología U-Pb y litogeoquímica de los principales segmentos del Batolito de la Costa[C]// Congreso Peruano de Geología, 19, Lima, Resúmenes ampliados. Lima: Sociedad Geológica del Perú, 101-105.

Wang, T.G., Zheng, L., Zhu, Y.P., Anthony, R., Zhao, Y.H., Yao, Z.Y. 2022. Precambrian supercontinent evolution and metallogeny of Australia. East China Geology, 43(03): 255-267.

Williams, G.E. 2023. Cyclic tidalites and seismites at a submarine hydrothermal system for a 2450 Ma banded iron formation,

Hamersley Basin, Western Australia. Australian Journal of Earth Sciences, 70(3): 323-331. DOI: 10.1080/08120099.2023.2150682.

Wilson, J. 1984. Geología de los cuadrángulos de Jayanca, Incahuasi, Cutervo, Chiclayo, Chongoyape, Chota, Celendín, Pacasmayo, Chepen. INGEMMET, Boletín[R]. Serie A: Carta Geológica Nacional, 38: 1-104.

Wu, H., Yu, Y.X., Xie, Y.F., Chen, S.P., Ma, Z.Z., Xu, X.L. 2015. Physical simulation on development of low- amplitude structures in slope zone of Oriente foreland basin, South America. Global Geology, 34(1): 178-186.

Xing, G.F., Qian, M.P., Huang, Z.Z., Zhu, Y.H., Li, C.H., Wu, B., Xu, M. 2016. Possible Storm Genesis Limestone in the Qixia Formation of Fuchun, Jiangxi Province. East China Geology, 37(02): F2.

Yao, C.Y., Guo, W.M., Liu, J.A., Li, H.W., Wang, T.G. 2024. Geochronology, petrogenesis and tectonic setting of the Eocene-Oligocene intrusive rocks in Chiclayo area, north of Peru. Acta Petrologica et Mineralogica, 43(1): 1-20. DOI: 10.20086/j.cnki.yskw.2024.0101.

Yuan, Y., Cai, P.C., Li, K.Z., Wei, A.J., Ye, T., Tan, X.C., Wang, X.Z. 2020. Characteristics of Lower Cretaceous seismites in the Rushan Basin, Shandong Province, China. Journal of Chengdu University of Technology (Science and Technology Edition), 47(3): 328-333,346.

Zeng, Y., Liu, Y., Guo, W.M., Shen, M.T., Xu, M. 2023. Magmatism and tectonic evolution of metamorphic basement in Carajás province of Brazil. Geological Survey of China, 10(5): 57-70.

Zhang, K.H., Wang, Y.R., Zhang, G.L., Xu, Tao., Xiong, W., Wang, S.Z., Ma, J., Sun, T.B. 2022. Discovery of Seismites in the Carboniferous Formation of the Shibei Sag (China) and Its Petroleum Geological Significance. Minerals, 12(12): 1560. DOI: 10.3390/min12121560.

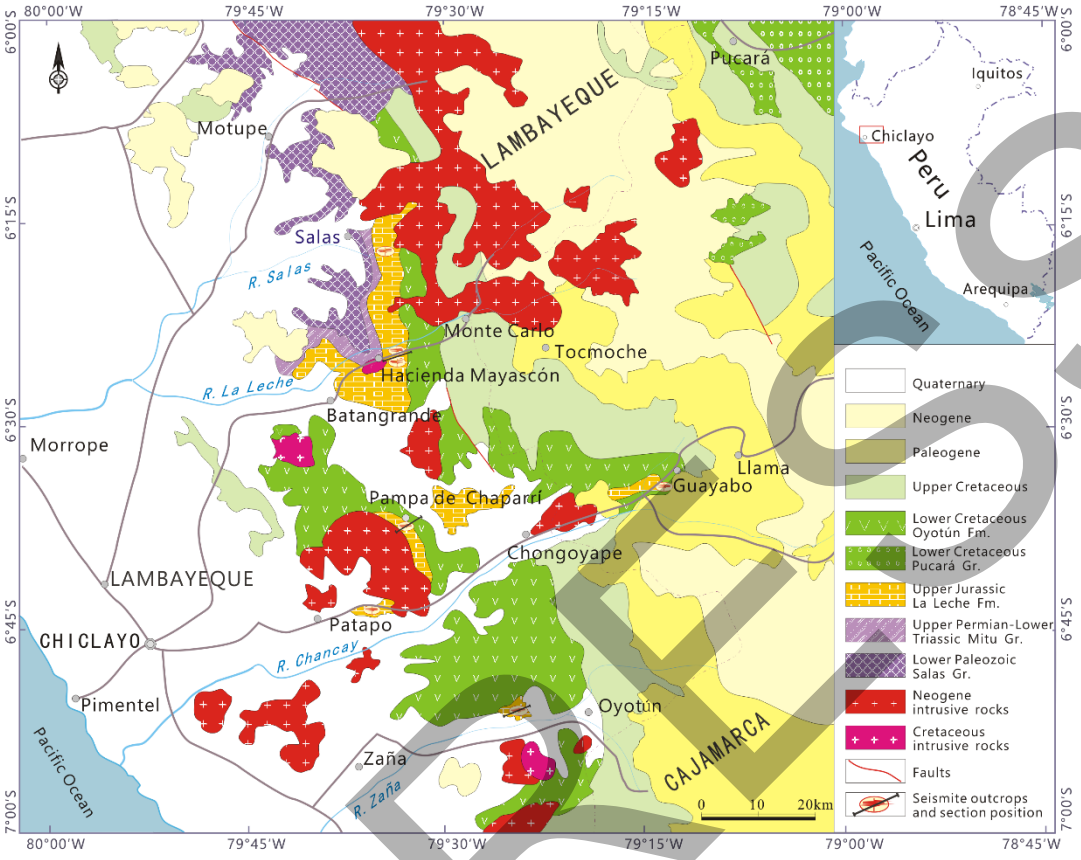

Fig. 1. Geological sketch map of the Chiclayo area in northern Peru (modified from Jaimes et al., 2023). Gray circles: towns and cities. Fm: Formation. Gr: Group.

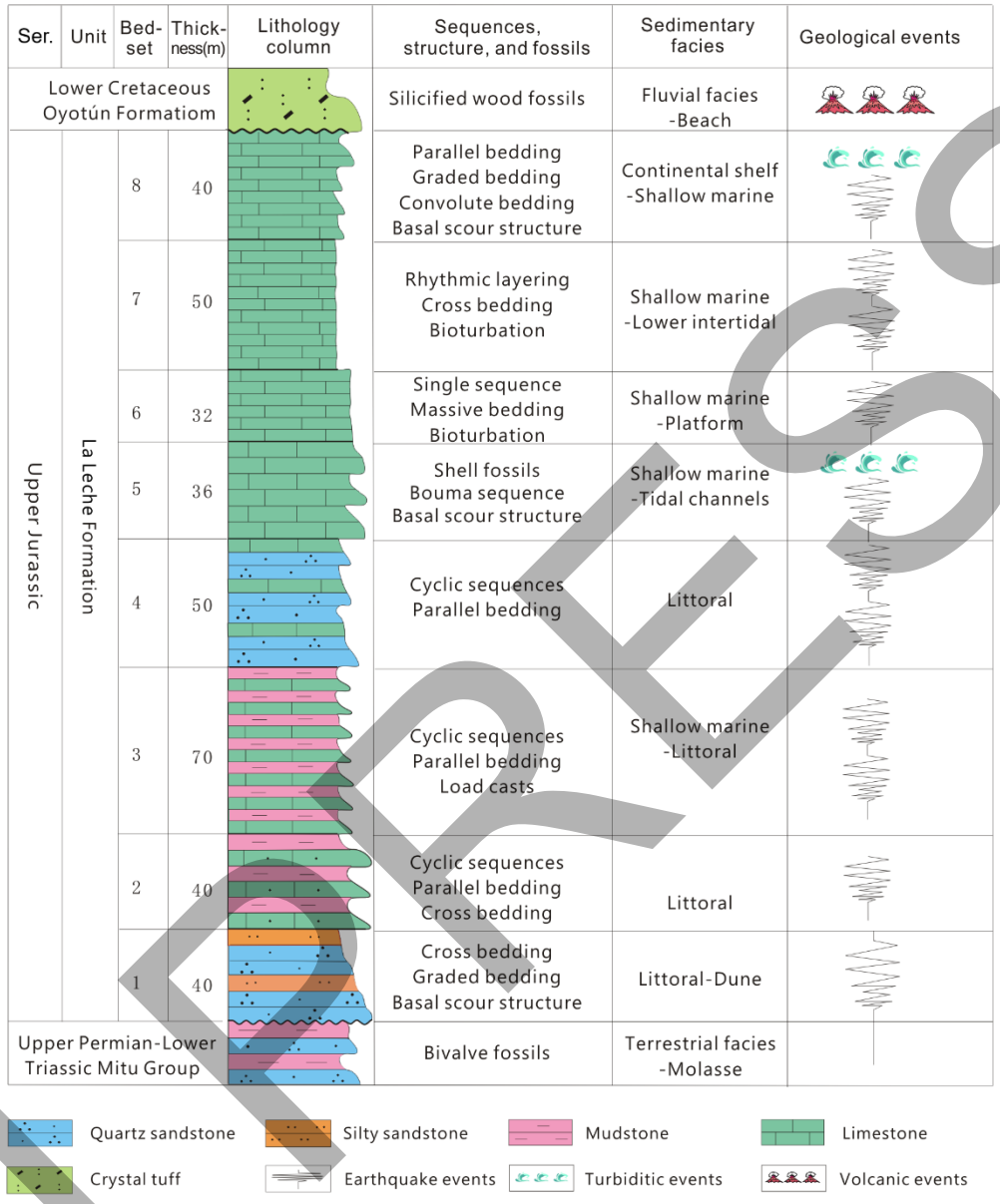

Fig. 2. Stratigraphic column and sedimentary environment of the La Leche Formation in the Chiclayo area.

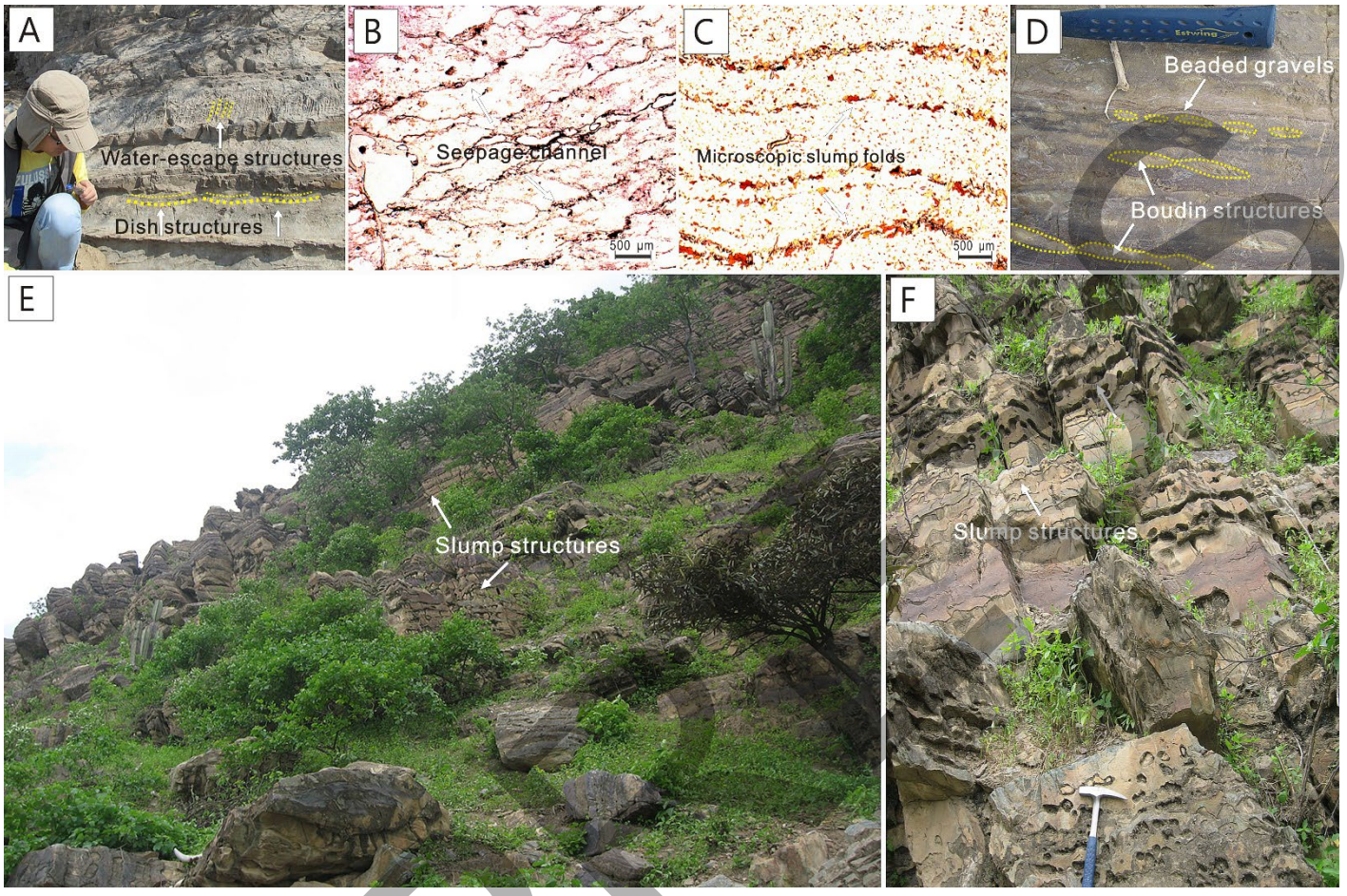

Fig. 3. Brittle deformation structures of the La Leche Formation in the Chancay River valley area (see figure 1 for location). **A.** Micro normal faults (yellow dotted lines) within the bed, arranged at a cm-scale, stepped lateral array. **B.** Microscopic normal faults within a limestone bed, filled with calcite (parallel nicols). **C.** Fractured breccias and fracture structures, showing multiple filling and fracturing events. **D.** Brittle fractures and Neptunian dikes, exhibiting multiple processes of breccia rupturing and dike filling; order of occurrence is 1-2-3-4.

Fig. 4. SSDS of the La Leche Formation in the Chancay and La Leche river valley areas. **A.** Water-escape and dish structures within the lamination (Chancay area). **B.** Microscopic seepage channel through which pore water escaped laterally (parallel nicols; La Leche area). **C.** Folding deformation microfeatures formed by liquefaction processes (parallel nicols; La Leche area). **D.** Beaded gravels and boudin structures (La Leche area). **E.** Slump structures (Bedset 8, La Leche area). **F.** Weathered slump structures (La Leche area).

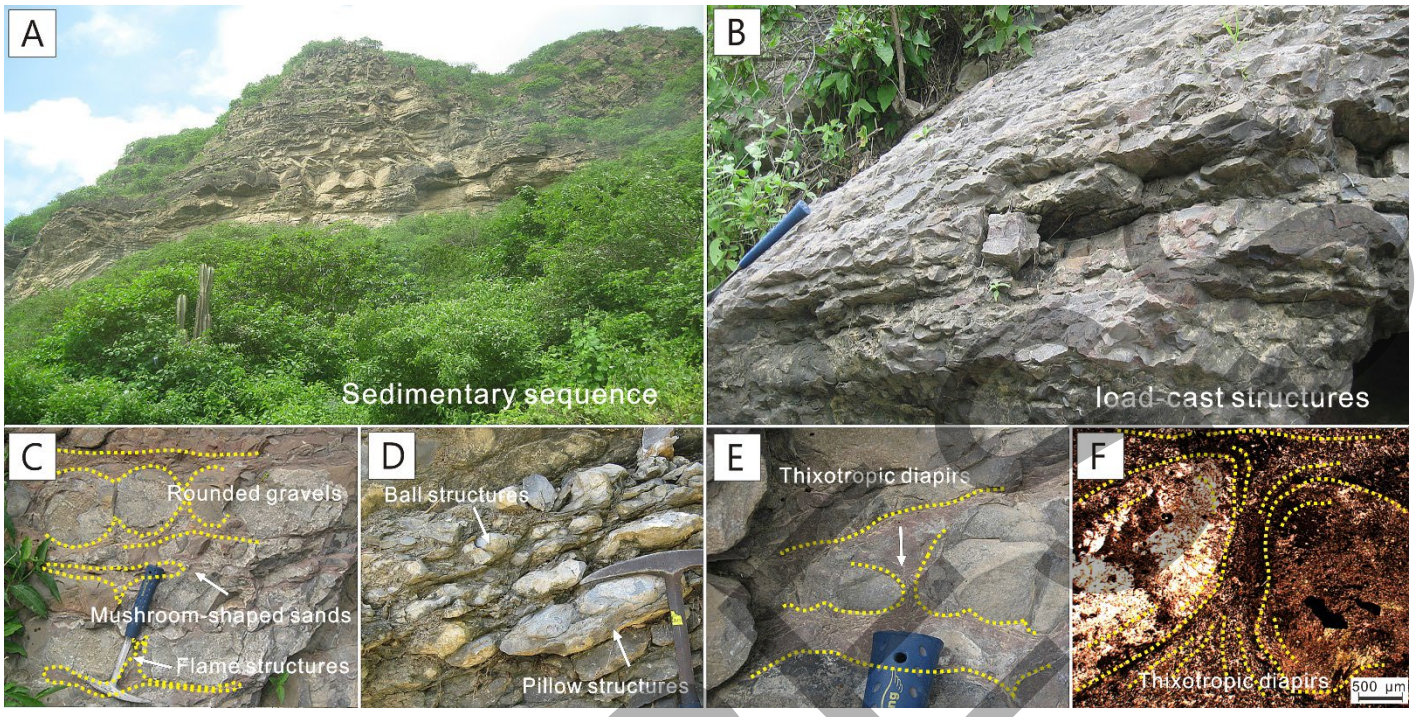

Fig. 5. SSDS of the La Leche Formation in the Chancay and La Leche River valley areas. **A.** Prospect of sedimentary sequence in the middle of the Chancay section. **B.** Interbedded sandy limestone and calcareous mudstone in the lower part of the La Leche section. **C.** Flame structures, mushroom-shaped sands, and self-fragmented breccias of load-cast structures (La Leche area). **D.** Juxtaposition of sand ball-and-pillow structure (Chancay area). **E.** Thixotropic diapir and flame structures (La Leche area). **F**. Microscopic thixotropic diapir structures (crossed nicols; La Leche area).

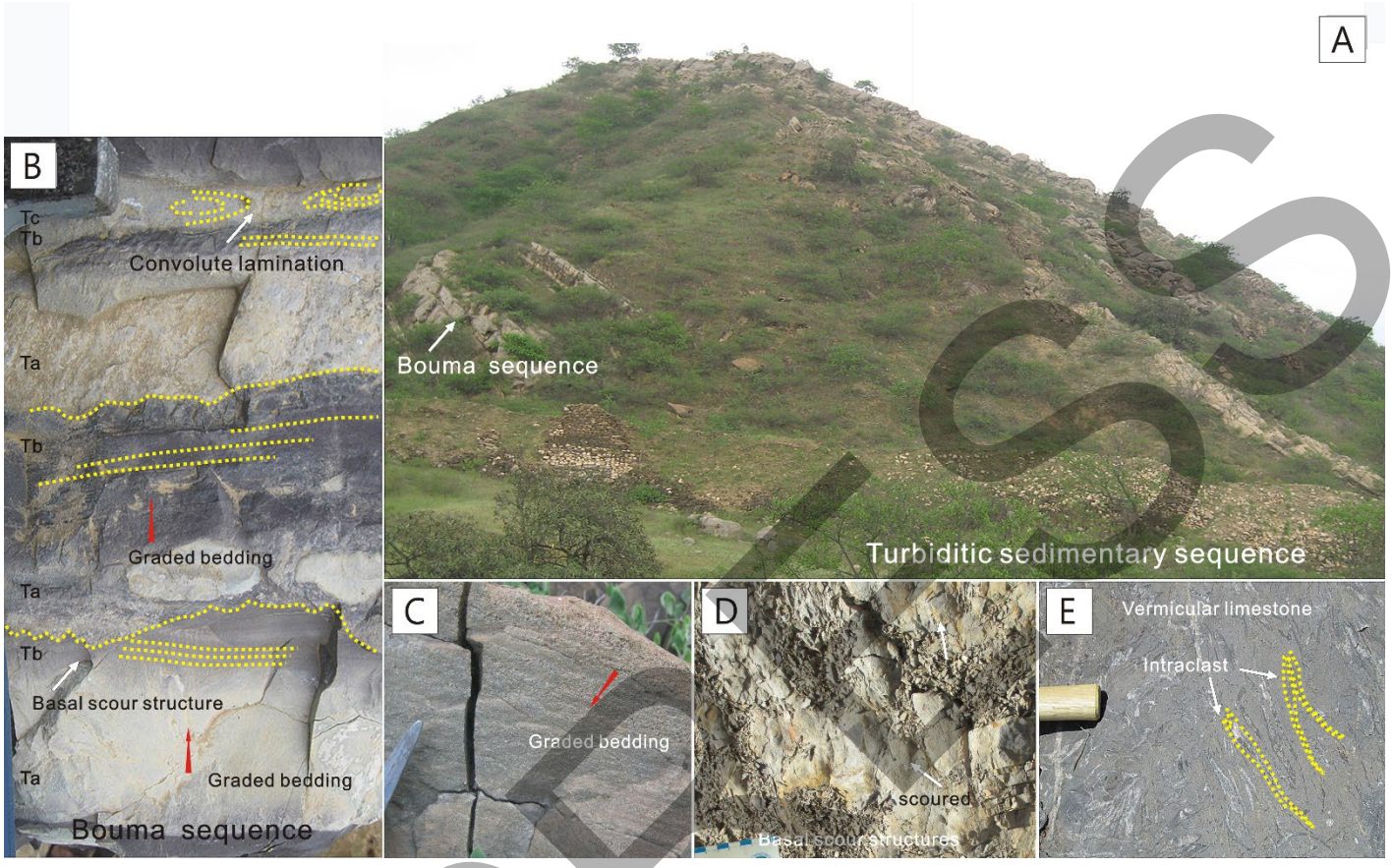

Fig. 6. Turbidite structures of the La Leche Formation in the Chiclayo area. **A.** Turbiditic sedimentary sequence, general view (Pampa del Chaparrí area). **B.** Incomplete Bouma sequence (La Leche area); Ta, Tb, and Tc being the depositional units within it. **C.** Graded bedding in sandstone (Pampa del Chaparrí area). **D.** Basal scour structures (Pampa del Chaparrí area). **E.** Vermicular limestone (Chancay area).

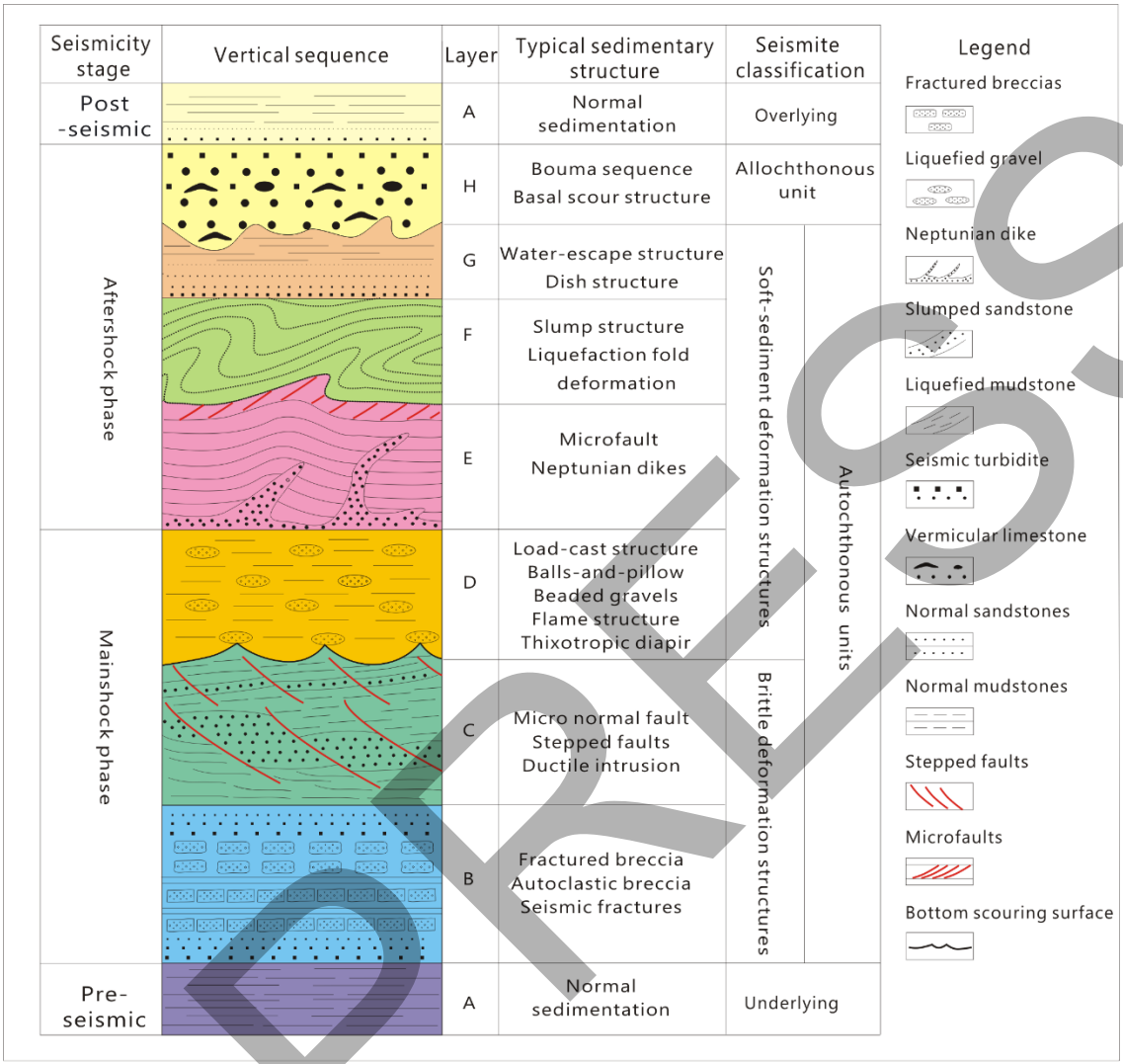

Fig. 7. Seismic sedimentary sequence of the La Leche Formation in the Chiclayo area.